

DESIGN AND CHARACTERIZATION OF GEOTEXTILES FOR HIGH PERFORMANCE APPLICATIONS

Refereed Journal Articles

- Elton, D. J., Mohamed, T., and Adanur, S., "BubblePoint and AOS Testing of Geotextiles", Proceedings of the Geosynthetics Conference, 2001, Portland, Oregon, Feb. 12-14, 2001.
- Adanur, S., and Liao, T., "Fiber Arrangement Characteristics and Their Effects on Nonwoven Tensile Behavior", Textile Research Journal, 69(11), 816-824, Nov. 1999.
- Liao, T., and Adanur, S., "Computerized Failure Analysis of Nonwoven Fabrics Based on Fiber Failure Criterion", Textile Research Journal, 69(7), 489-496, July 1999.
- Liao, T., and Adanur, S., "A Novel Approach to Three Dimensional Modeling of Interlaced Fabric Structures", Textile Research Journal, 68(11), November 1998, pp. 841-847.
- Adanur, S., and Liao, T., "Computer Simulation of Mechanical Properties of Nonwoven Geotextiles in Soil-Fabric Interaction", Textile Research Journal, 68(3), March 1998, pp. 155-162.
- Liao, T., Adanur, S., and Drean, J., "Predicting the Mechanical Properties of Nonwoven Geotextiles with the Finite Element Method", Textile Research Journal, Vol. 67, No. 10, October 1997, pp. 753-760.
- Basu Mallick, S., Elton, D. J., and Adanur, S., "An Experimental Characterization of Soil-Woven Geotextile Interface in Large Box Pullout Tests", Geosynthetics, March 1997, pp. 927-940.
- Mallick, S. B., Zhai, H., Adanur, S., and Elton, D. J., "Pullout and Direct Shear Testing of Geosynthetic Reinforcement: A State of the Art Report", Transportation Research Record, No. 1534, Soils, Geology and Foundations, Transportation Research Board, National Research Council, National Academy Press, Washington, DC, 1996, pp. 80-90.
- Zhai, H., Basu Mallick, S., Elton, D., and Adanur, S., "Performance Evaluation of Nonwoven Geotextiles in Soil-Fabric Interaction", Textile Research Journal, Vol. 66, No. 4, April 1996, pp. 269-276.

Presentations with Conference Proceedings

- Elton, D. J., Howie, D. L., and Adanur, S., "Bubblepoint Testing of Nonwoven Geotextiles", Proceedings of the 37th Symposium on Engineering Geology and Geotechnical Engineering", 2002.
- Elton, D. J., and Adanur, S., "Varying Pore Sizes in Hydroentangled Geotextiles", Proceedings of the Techtexil North America International Trade Fair for Technical Textiles and Nonwovens, Vol. 3, March 22-24, 2000, Atlanta, GA.

- Mallick, S. B., Elton, D. J., and Adanur, S., "A New Approach in Modeling of Soil-Geotextile Interface Behavior in Pullout Tests", Proceedings of the Sixth International Conference on Geosynthetics, March 25-29, 1998, Atlanta, GA.
- Basu Mallick, S., Elton, D. J., and Adanur, S., "An Experimental Characterization of Soil-Woven Geotextile Interface in Large Box Pullout Tests", Proceedings of the Geosynthetics '97, Long Beach, CA, March 1997, pp. 927-940.
- Adanur, S., Mallick, S., and Zhai, H., "Analysis of Geotextile-Soil Interaction in Pull-Out Tests", Proceedings of the IS Kyushu '96, International Symposium on Earth Reinforcement, Fukuoka, Japan, November 1996.
- Adanur, S., Mallick, S. B., and Zhai, H., "Design and Characterization of Geotextiles for High Performance Applications", Proceedings of the Hi-Tech Textiles Exhibition and Conference, Textile World and INDA, Greenville, SC, July 1995.
- Mallick, S. B., and Zhai, H., "A Laboratory Study on Pull-out Performance of Woven Geotextiles", Geosynthetics '95 Conference Proceedings, Nashville, TN, February 1995. This student paper, directed by Dr. Adanur and Dr. Elton, was one of the 6 papers accepted for the conference.

Acknowledgment

This work is supported by the United States Department of Commerce Grant No. 99-27-07400 through the National Textile Center, which is appreciated.

Design and Characterization of Geotextiles for High Performance Applications

Sabit Adanur - Textile Engineering, Auburn University

David Elton - Civil Engineering, Auburn University

Post-doctoral fellow: Tianyi Liao

PhD Student: Sumita Basu Mallick

Goal

To analyze the soil-geotextile interface and develop new geotextile product(s) based on the scientific understanding of this interaction.

Abstract

Substantial amount of work has been done in this project in engineering applications of geotextiles. We analyzed the geotextile-soil interaction theoretically and experimentally in pull out tests. We used both woven and nonwoven geotextiles. The results showed that a new type of geotextile needs to be developed to improve the shortcomings of woven and nonwoven geotextiles.

1. Introduction

Geotextiles are widely used with soil structures in the field of geotechnical engineering. In these applications geotextile compensates for the obvious weakness of soil in withstanding tensile stress through the geotextile's strength and soil/geotextile interaction. The necessity of tests on geotextiles to study their suitability for a particular application is becoming more and more important as the variety of geotextiles and their use in geotechnical works have been increasing.

The pullout test is a common test in determining the strength and deformation parameters between geotextile and soil in the design of reinforced earth structure. In this study, we are developing new finite element models for woven and nonwoven geotextiles. The objective is to obtain information about the deformation, stress and strain distribution within the sample during pullout tests, and the influences on constituent fiber properties and structure-related parameters of geotextiles.

2. Theoretical and Experimental Work for Nonwoven Geotextiles in Pullout Tests

First, we described the finite element's constitutive matrix and stiffness matrix from the knowledge of stress-strain behavior of fabric's constituent fibers and their distribution of fiber orientation angles. Then we calculated the deformation, stress and strain distribution at any point along the embedment length, as well as the pullout load versus displacement curves. Finally, we

conducted pullout tests for several nonwovens and made comparisons between the calculated and experimental results.

Finite Element Formulations: Several assumptions are made for the model. Basically, each fiber layer made up of parallel fibers can be considered as a thin sheet of orthotropic material. Based on the stress strain behavior of biaxially stressed orthotropic materials, we can deduce the equilibrium equation for each finite element as follows:

$$\begin{Bmatrix} F_1 \\ F_2 \\ F_3 \\ F_4 \\ F_5 \\ F_6 \end{Bmatrix} = \frac{T}{2} \cdot \begin{bmatrix} b_1 & 0 & c_1 \\ 0 & c_1 & b_1 \\ b_2 & 0 & c_2 \\ 0 & c_2 & b_2 \\ b_3 & 0 & c_3 \\ 0 & c_3 & b_3 \end{bmatrix} \cdot \left(\sum_{i=1}^N \frac{G}{r \cdot T} \cdot \Phi_{\beta_i} \cdot E_f \cdot \begin{bmatrix} \cos^4 \beta_i & \sin^2 \beta_i \cdot \cos^2 \beta_i & \sin^3 \beta_i \cdot \cos \beta_i \\ \sin^2 \beta_i \cdot \cos^2 \beta_i & \sin^4 \beta_i & \sin^3 \beta_i \cdot \cos \beta_i \\ \sin^3 \beta_i \cdot \cos \beta_i & \sin^3 \beta_i \cdot \cos \beta_i & \sin^2 \beta_i \cdot \cos^2 \beta_i \end{bmatrix} \right) \cdot \begin{bmatrix} b_1 & 0 & b_2 & 0 & b_3 & 0 \\ 0 & c_1 & 0 & c_2 & 0 & c_3 \\ c_1 & b_1 & c_2 & b_2 & c_3 & b_3 \end{bmatrix} \cdot \begin{Bmatrix} U_1 \\ U_2 \\ U_3 \\ U_4 \\ U_5 \\ U_6 \end{Bmatrix}$$

where $F_1 \dots F_6$: the force components at nodal points; $b_1, b_2, b_3, c_1, c_2, c_3$: algebraic constants; β_i : fiber orientation angle in the i^{th} layer; Φ_{β_i} : relative frequency of fiber in the i^{th} layer; E_f : fiber modulus; $U_1 \dots U_6$: displacement component at nodal points; N : number of layers in the fabric; G : weight per square meter of the fabric; T : thickness of the fabric; ρ : specific gravity of fiber.

Acting Force and Constraint Conditions : The soil/geotextile interactions are mainly contributed by two factors: the interlocking of grain particles in fabric voids and the soil-fabric surface friction. These two factors act together to transfer shear stresses from reinforcement to soil. In this study, these shear stresses are realized by introducing a set of parallel forces acting on the fabric at the mesh nodal points. The direction of these forces is opposite to the direction of fabric displacement (Figure 1).

In order to simulate the pullout tests, the boundary constraint conditions are chosen in such a way that one lateral boundary of sample remains stationary, and the other three remaining boundaries were left to move. The nodal displacements in the stationary boundary were specified to be zero in the computational procedure. Therefore, no vertical or horizontal movement is allowed for nodes on the stationary side.

Solution of System Equilibrium Equation: The system equilibrium equation can be established based on the single element equilibrium equation, fabric sample configuration and the mesh lines dividing the sample. Once the boundary constraint conditions and the acting forces are defined, the system equilibrium equation can be solved and the nodal displacement throughout the entire sample can be obtained. The knowledge of nodal displacements, in turn, can be used to determine the fabric deformation and configuration. It is also possible to use the calculated values of the nodal displacement to calculate other parameters of interest, such as the stresses and the strains in every element, the fabric Poisson's ratio, and the pullout force acted on the fabrics. As a result, we can predict the deformation behaviors and other relative properties of nonwoven geotextiles in soil geotextile interaction from the knowledge of the stress-strain behavior of constituent fibers, the distributions of fiber orientation angles and the constraint conditions.

Computational Method: Experimental data regarding the fiber physical and mechanical properties and fiber web structure parameters are supplied to the main program as the initial data. The size and shape of the sample, the number of elements and the spatial coordinates of all nodal points within the fabric are also entered. Meanwhile, the boundary constraint conditions, the acting forces and their exerting points are fed into the calculation program as well.

After running the fiber modulus approach program and the force bearing area determination program, a set of computed results are produced in digital or graphical form. The output results include the deformation shape of geotextile, element stresses, element strains, and pullout load versus displacement curves.

The program was written in C Language and run on Sun computer station under the UNIX system, while the graphical output was produced by Mathematica™ and Xplot™ software. The cpu time used to generate the full data was less than 15 minutes in the Engineering Computer Center at Auburn University.

Experimental Procedures: Two kinds of nonwoven geotextiles supplied by LINQ Industrial Fabrics, Inc., and Hoechst Celanese Corp. were used in this study. Fabric A: GTF 180EX made of polypropylene, needle punched, 213.6 grams per square meter, 2.03 mm thickness. Fabric B: Trevira® 011/250 made of polyester, spunbonded, 254.3 grams per square meter, 2.41mm thickness.

A large pullout box in conjunction with the Instron Material Testing system was used for the pullout test. Figure 2 shows the schematic of the experimental system. The box dimensions are 61 cm (width) X 91.5 cm (length) X 45.7 cm (height). In the middle of the front side, there is a horizontal opening through which the fabric is pulled. The force-displacement data were recorded with a data acquisition system controlled by a microcomputer. Loading was stopped if the front end displacement exceeded 125 mm or if the geotextile failed in tension.

Results and Discussion: The model fabrics were strained at 10% increments of shear force acting from the front end of the fabric until the shear forces acted on the entire area of contact between the fabric and sand.

The distributions of the strains in transverse direction, ϵ_x , within fabric A in different pullout steps are shown in Figure 3. From these figures, we can find the forming and developing procedures of the lateral contractions of the sample during pullout test. At the beginning of the test, the lateral contraction occurs at two boundaries of the sample near clamp, which are presented by the two darkest areas in Figure 3 (a). As the pullout load increased, the contraction regions developed toward the center portion of the fabric, and extended in the direction of free end. The imperfect symmetry of the lateral contraction observed in Figure 3(b) may result from the imperfect symmetric distribution of fiber orientation within the fabric. Figure 3 (c) shows the lateral contraction contour within the fabric in the final situation. The contractions gradually decreases to zero at the free end and at the clamp due to the constraints imposed by jaws. Such behavior is very similar to the deformation of fabrics observed during pullout tests.

The distributions of the stresses in longitudinal direction within the fabric during pullout tests are plotted in Figure 4. The figures, the stress and the corresponding elongation along the anchorage length of the geotextile are developed progressively from the front end to free end. In Figure 4 c, the stresses reach to the free end and all the region within the fabric is subjected to

shear resistance from the sand. This point may be called the maximum shear force. Beyond this point, the fabric will slide if the pullout load continues to increase. The stresses in the regions near the clamped boundary are much higher than the other parts, particularly in two corners of the sample. This explains the reason why the breaks usually occur near the clamps of the pullout test machine.

Figure 5 shows the contour plots of the shear strains of the geotextile sample A during the pullout test. The dark regions in the figures represent high shear deformation in an anti-clockwise direction, and the white regions represent high shear deformation in a clockwise direction. The shear strains develop toward the free end with the progress of the pullout test, but they always concentrate at the clamped boundary of the fabric.

The experimental pullout load versus displacement curves and those computed from the models under different normal pressures for fabric A are plotted in Figure 6. The difference in normal pressure level could cause a large variation in the predicted pullout load. A high value of normal pressure results in high shear forces acted on the fabric. Therefore, the fabric under high pressure experiences a large deformation and stress. Good agreement was found between theoretical curves and experimental values.

3. Theoretical and Experimental Work for Woven Geotextiles in Pullout Tests

Three 2D plane strain nonlinear models were selected as trial runs to simulate the stress-strain behavior of a woven geotextile subjected to a pullout load. Model 1 (Figure 7) was structured with small number of finite elements to represent the complete experimental system with soil and the geotextile. For model 1, linear elements were used to represent the geotextile. Model 1 was tested for initial pullout displacement of 40 mm and for this displacement region stress-strain relationship for soil and geotextile materials were considered to be linearly elastic. For the correct simulation of the stick-slip behavior of the interface, geometric nonlinearity was incorporated in the model.

Model 2 (Figure 8) is a full scale version of model 1 with finer mesh. Stress-strain relationship for geotextile material is modeled as nonlinear-elastic. Model 3 (Figure 9) simulates the soil-geotextile interface region with two thin layers of soil, on top and bottom of the geotextile sheet. Very small (1 mm by 2 mm) quadrilateral elements were selected to represent the geotextile and soil. Gap elements are used to connect the soil and geotextile elements and to simulate the stick-slip behavior of the interface. Both geometric and material nonlinearity were incorporated in the model.

Elements and parameters used for Model 1

Inside the pullout box, soil was modeled using a nonlinear, four node, isotropic, quadrilateral element. The material properties used for the quadrilateral elements are: Modulus = 100 MPa, $\nu=0.3$, $\phi=32^\circ$, $c=0$ (dry sand).

Soil-geotextile interface was modeled with 10 isotropic gap elements. A transverse shear stiffness was used to simulate the frictional force at the interface. In this case interface was modeled as a closed gap before the application of any horizontal load. As the load is applied, the stick-slip behavior of the interface was examined with the behavior of gap element under the specified loading condition. Parameters selected as the properties of the gap elements are: axial

stiffness= 80.E+7 N/m, transverse stiffness= 9.E +7 N/m, coefficient of static friction= 3.0, coefficient of kinetic friction= 0.1

Reinforcement was modeled with four one dimensional rod element with no bending stiffness. Variable modulus was selected for the elements. Parameters selected as the properties of the rod elements are: thickness= 0.001m, modulus= 5250 kN/M. Normal Pressure was 7 kPa and the pullout displacement was 40 mm (10 % increments).

Results: Figure 10 shows the displacement measured and calculated along the length of the geotextile. A considerable difference between the measured and calculated values was noticed at the load application point. As the measured displacement values are considerably higher than the calculated values only at the load application point, it can be derived from the comparison of the results that the geotextile material behaves nonlinearly close to load application point.

Figure 11 shows the calculated and measured load-displacement behavior at the front end of the geotextile. From the output it was observed that the calculated load response of the geotextile at different displacement levels are very close to the load measured during the experiment. Calculated loads are slightly higher than the measured load at all displacement levels. Figure 10 shows that the measured displacements at the front end of the geotextile (gage # 3, Figure 12) are higher than the calculated displacements. Therefore it can be concluded that a less stiff element with nonlinear material properties is needed to represent the front end of the geotextile.

Figure 13 shows the calculated pullout resistance along the length of the geotextile. From the results it can be noted that the pullout resistance obtained for element number two is smaller than that of the element number one. This behavior is probably related to the modulus value selected for the element. As the pullout resistance sharply increases from element 3 to element 4, nature of the load response graph shows a need for nonlinear modeling of the geotextile material close to load application point.

From the force-displacement output of gap elements it was observed that up to 15 mm displacement, all ten gap elements were sticking to the rod elements and no slip was calculated at the interface. From 15 to 40 mm displacement, gap element 5 and 10 (both at the load application point) starts slipping with kinetic friction. No sliding was observed from the analysis.

4. Conclusions

Finite element models have been developed and utilized for prediction of pullout load versus displacement curves of woven and nonwoven geotextiles. The calculated results of stress and strain distribution within the geotextile in soil-fabric interaction demonstrate the mechanical behavior of geotextiles buried under soil more clearly. A good agreement between the experimental results and those from the model, makes it possible to produce optimum geotextile for various applications by selecting the fibers with appropriate properties and designing proper fiber web structure and manufacturing processes. It is concluded that a new type of geotextile is needed which will optimize the properties of woven and nonwoven geotextiles.

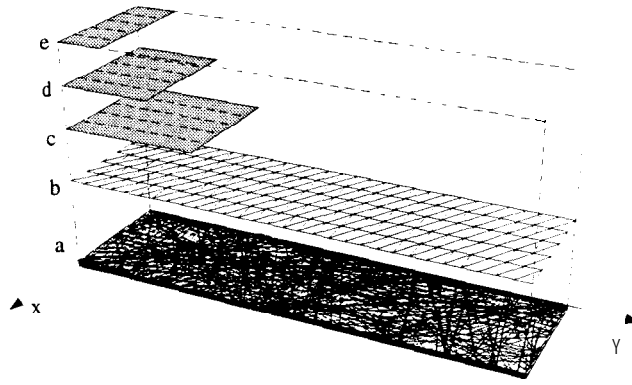


Fig. 1 The finite element mesh and shear forces. a. nonwoven geotextile model; b. finite element mesh; c,d and e. shear forces acting at nodal points at different pullout stages.

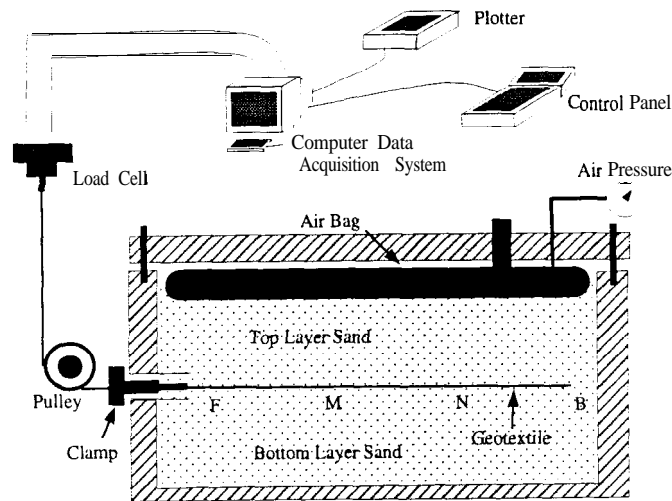


Fig. 2 Schematic of geotextile pullout test device

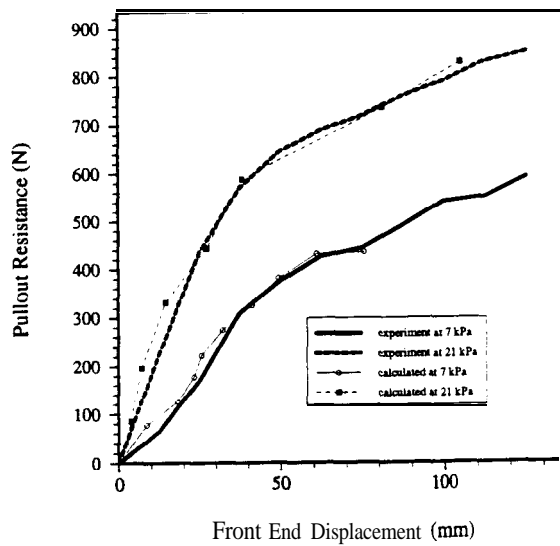


Fig. 6 The experimental pullout load versus displacement curves and those computed from the model for fabric A at normal pressure levels of 7 kPa and 21 kPa

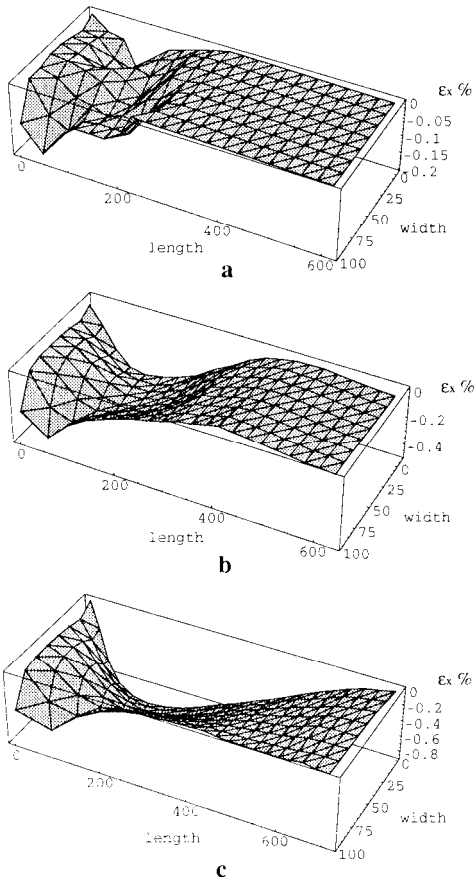


Fig. 3 The distribution of the strains in transverse direction, ϵ_x , within fabric in different pullout stages. a. Rarea=30%; b. Rarea=60%; c. Rarea=100% .

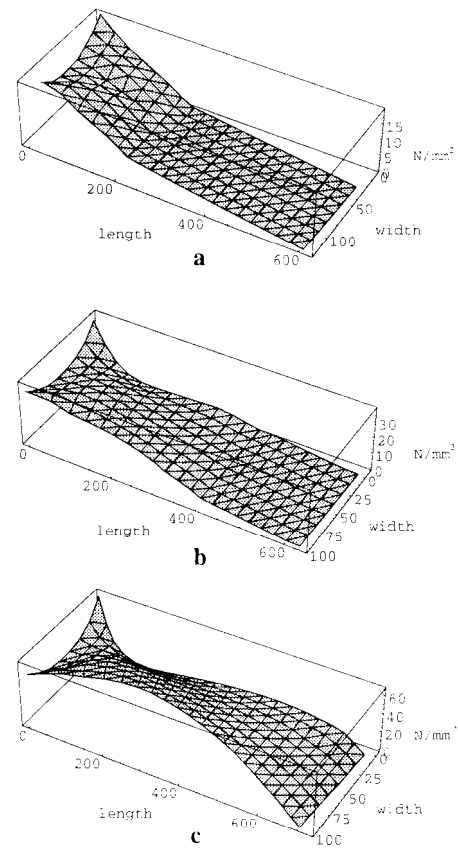


Fig. 4 The distributions of the stresses in longitudinal direction, σ_y , within fabric A in different pullout stages. a. Rarea=30%; b. Rarea=60%; c. Rarea=100%

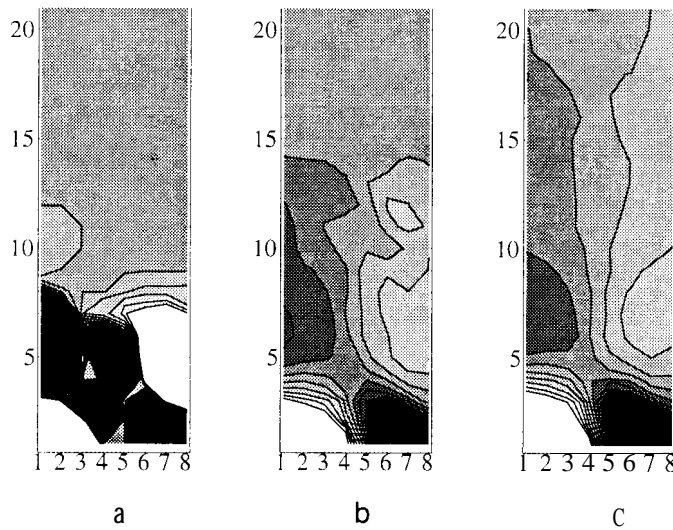


Fig. 5 The contour plots of the shear strains, γ_{xy} , within fabric A in different pullout stages. a. Rarea=30%; b. Rarea=60%; c. Rarea=100% .

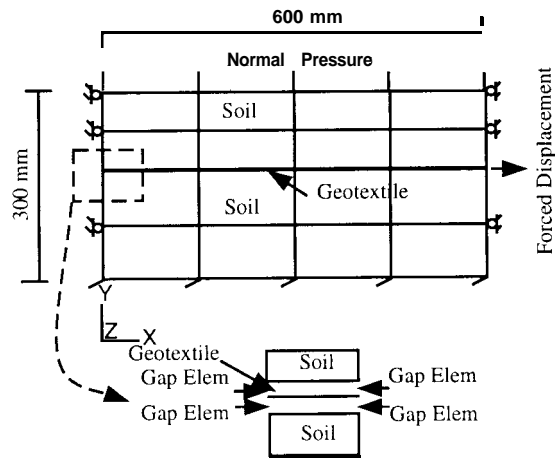


Figure 7 Finite element Model 1

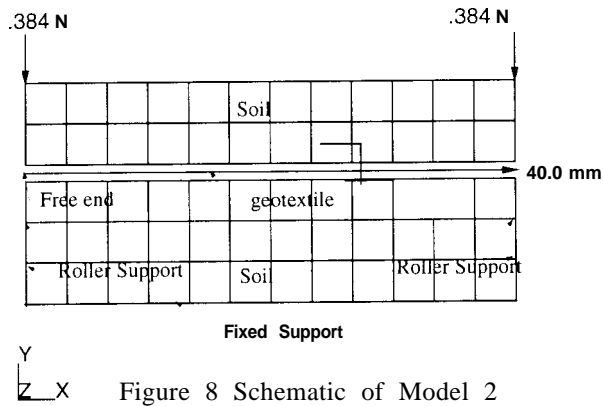


Figure 8 Schematic of Model 2

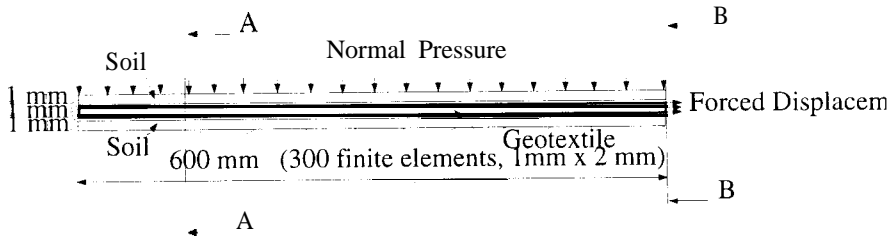
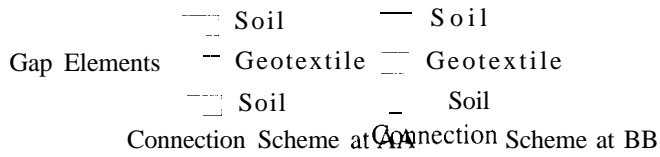


Figure 9. Schematic of Model 3

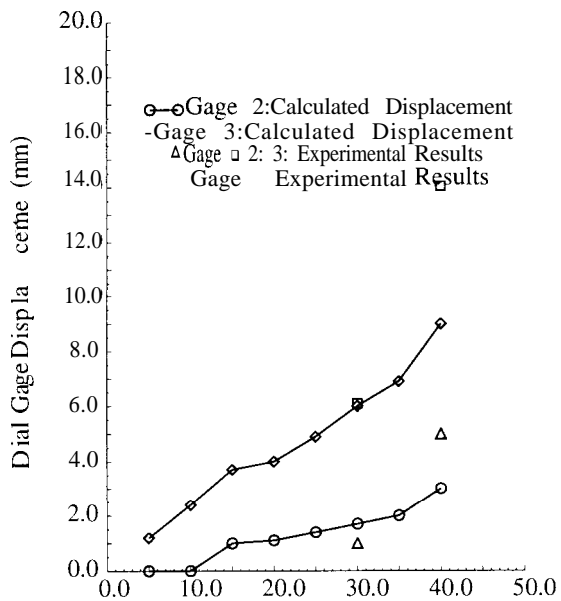


Figure 10 Calculated and Measured Displacements along the Length of the Geotextile

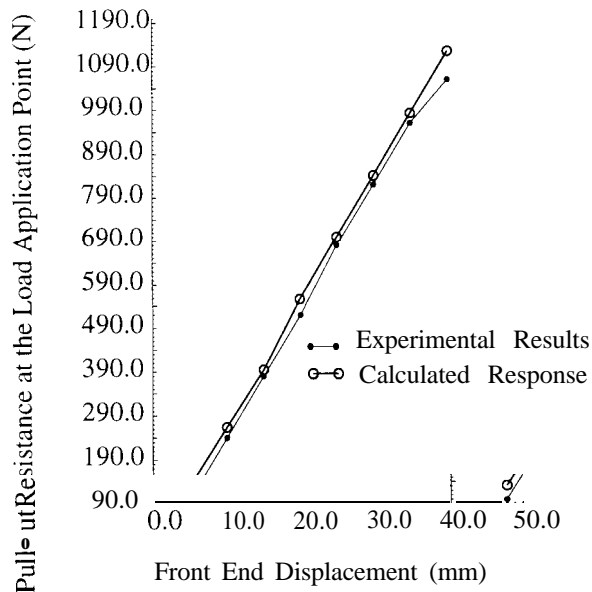


Figure 11 Calculated and Measured Load-Displacement behavior

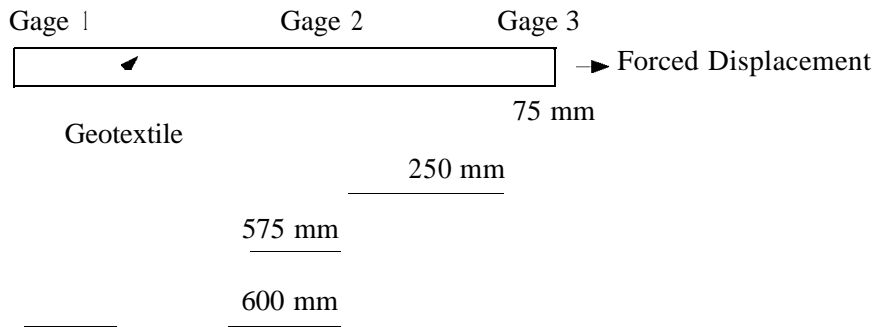


Figure 12 Positions of Dial Gages 1, 2 and 3

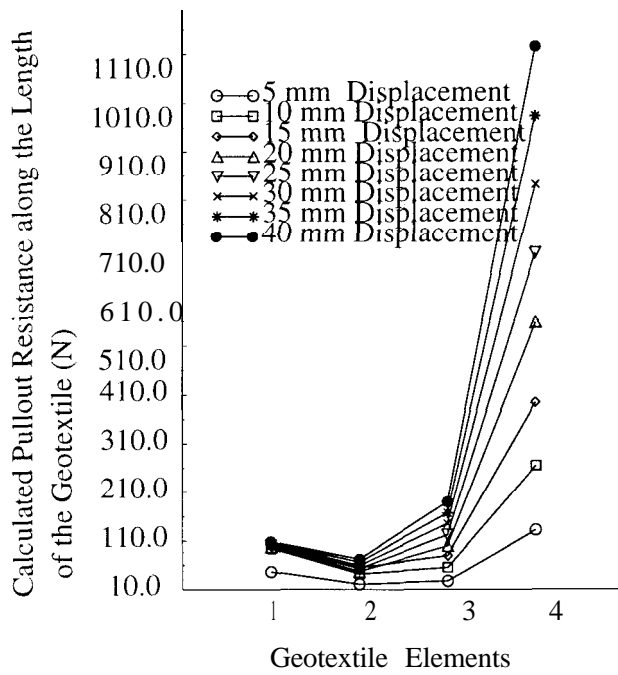


Figure 13 Pullout Resistance along the Length of the Geotextile